Recent QCD results from ATLAS

Javier Llorente, on behalf of the ATLAS Collaboration

PHENO 2015, Pittsburgh

4th - 6th May 2015

Outline of the talk

1. Measurements of soft QCD phenomena:
    1. Underlying event in Z boson events.
    2. Polarisation of the Λ hyperons produced in minimum bias events.
    3. Characterisation of two-particle Bose-Einstein correlations.

2. Measurements of hard scattering processes:
    1. Di-jet production with large rapidity gaps in the hadronic activity.
    2. Inclusive (1,2,3)-jet differential cross sections.
    3. Isolated, high-p_T inclusive photon cross section.
    4. Jet shapes in $t\bar{t}$ events.

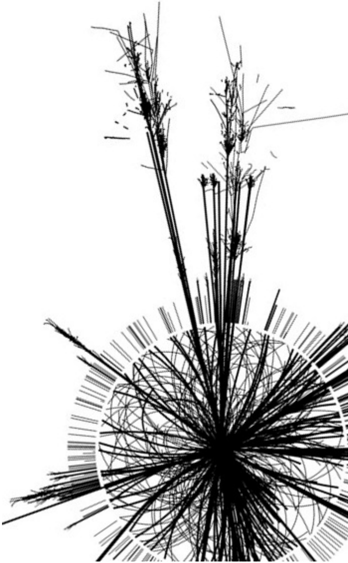

1. Soft QCD measurements

- UE: All additional hadronic activity not arising from the hard scattering.
- Measured track observables: $\sum p_T$, N_{ch} per $\delta\eta \times \delta\phi$ unit, average mean p_T.
- Three regions considered depending on $\Delta\phi$ to the direction of the Z boson: Toward, away, transverse.

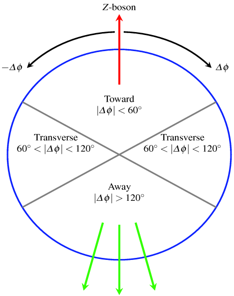

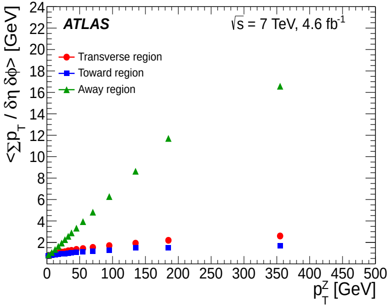

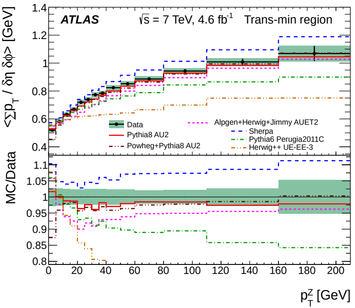

- The distribution of $t = \cos\theta^*$ follows $g(t, P) = \frac{1}{2}(1 + \alpha P t)$.
- Signal and background fractions obtained from invariant mass fits.

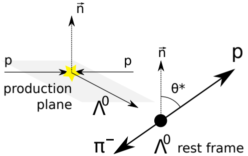

- The extraction of the polarisation follows the method of moments:

$$\chi^2(P, E_{bkg}) = \sum_{i=1}^{3} \frac{[E_i - E_i^{exp}(P, E_{bkg})]^2}{\sigma^2_{E_i}}$$

where $E_i^{exp} = f_i^{sig}\{E_i^{MC}(0) + [E_i^{MC}(1) - E_i^{MC}(0)]P\} + (1 - f_i^{sig})E_{bkg}$

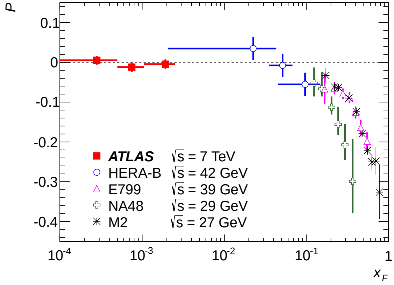

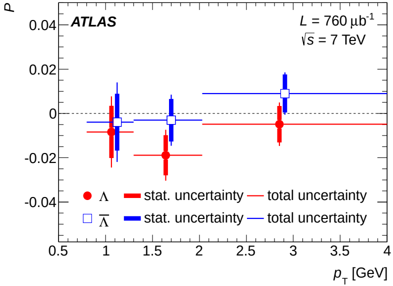

- Correlations in $Q^2 = -(p_1 - p_2)^2$
- $R_2(Q) = \frac{\rho^{++}_{--}(Q)}{\rho_{+-}(Q)} \Big/ \left(\frac{\rho^{++}_{--}(Q)}{\rho_{+-}(Q)}\right)_{MC}$
- Parameterisation in terms of the function $\Omega(Q; R, \lambda) = \lambda e^{-RQ}$
- Data corrected for Coulomb effects

$$G(Q) = \frac{2\pi\zeta}{e^{2\pi\zeta} - 1}; \quad \zeta = \pm\frac{\alpha m_\pi}{Q}$$

- Bins in n_{ch} and $k_T = |\vec{p}_{T1} + \vec{p}_{T2}|/2$

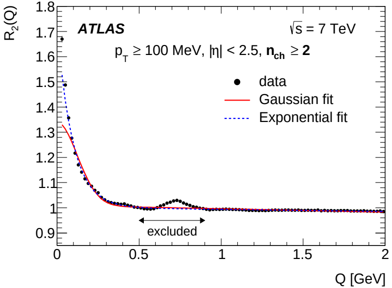

- $\sqrt{s} = 900$ GeV and 7 TeV data.

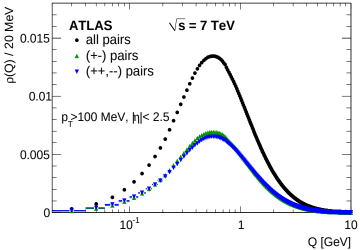

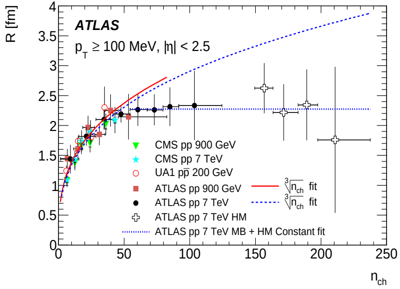

2. Hard QCD measurements

- Observables: Gap fraction $\sigma_{jj}(Q_0)/\sigma_{jj}$, $\langle N_{jet}\rangle$ in rapidity gap, $\langle cos(\pi - \Delta\phi)\rangle$. Dependence on Δy and the average $\overline{p_T} = (p_{T1} + p_{T2})/2$.
- Kinematics: $p_{T1} > 60$ GeV, $p_{T2} > 50$ GeV for the dijet system.
- BFKL-sensitive for large Δy.
- Comparisons with POWHEG and HEJ.

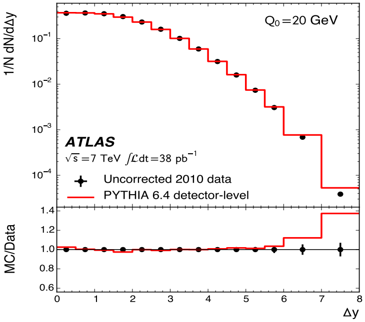

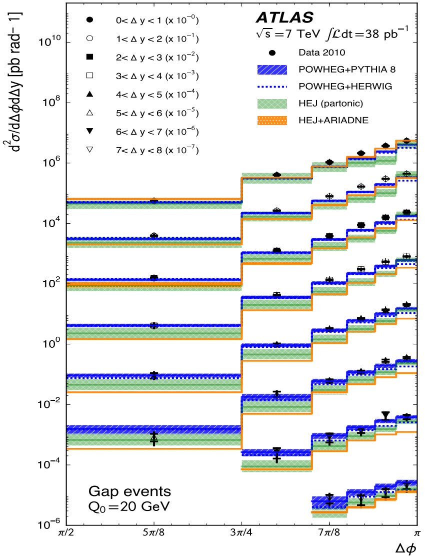

The amount of decorrelation is increased at high Δy and low $\overline{p_T}$

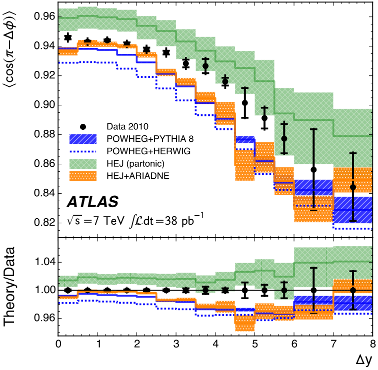

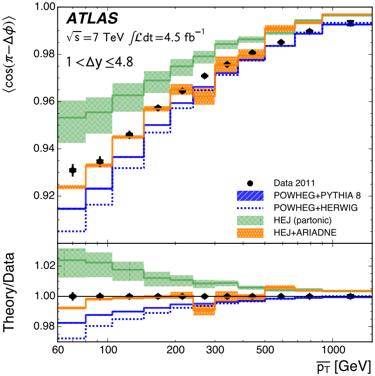

2.2 Inclusive jet cross section. JHEP 02, 153 (2015)

- Double-differential cross section as a function of the jet p_T and rapidity. $\sqrt{s} = 7$ TeV, $\int Ldt = 4.5$ fb^{-1}.
- Two jet radii are used: $R = 0.4$ and $R = 0.6$. Jets with $p_T \geq 100$ GeV, $|y| < 3$ considered.
- Comparison with NLO predictions corrected for EW and NP effects. Several PDFs investigated.

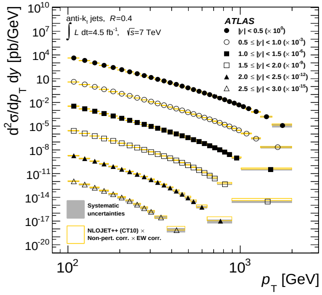

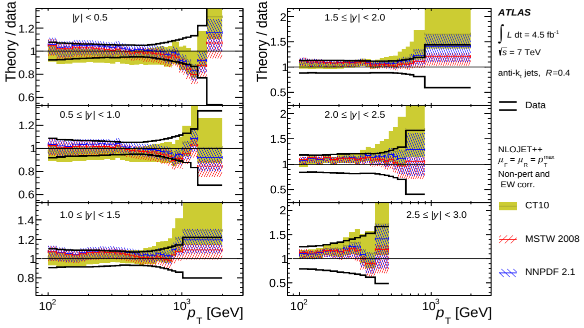

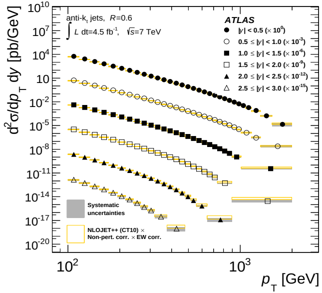

2.3 Dijet cross section. JHEP 05, 059 (2014)

- Double-differential cross section as a function of m_{12} and $y^* = |y_1 - y_2|/2$. $\sqrt{s} = 7$ TeV, $\int Ldt = 4.5$ fb^{-1}.
- Kinematical requirements: $p_{T1} \geq 100$ GeV, $p_{T2} > 50$ GeV and $|y| < 3$
- Comparison with NLO predictions corrected for EW and NP effects. Several PDFs investigated.

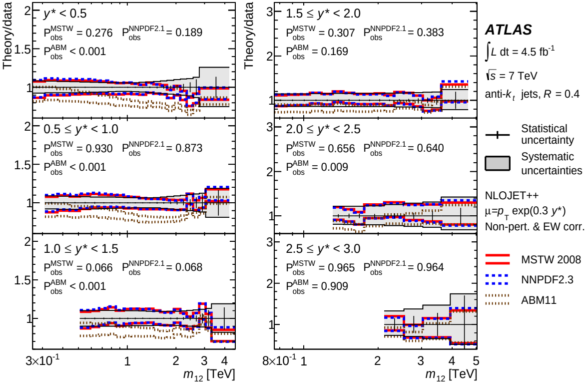

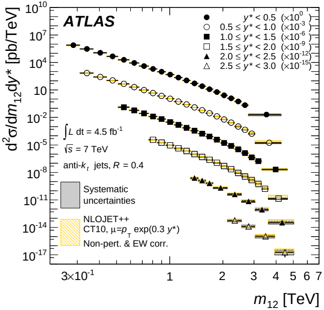

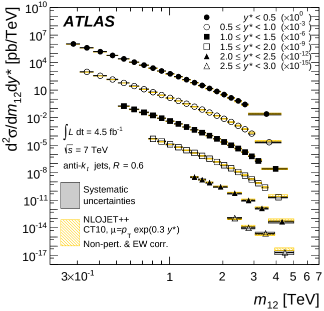

2.4 Three-jet cross sections. arXiv:1411.1855 [hep-ex]

- Double-differential cross section as a function of m_{jjj} and $|Y^*| = |y_1 - y_2| + |y_2 - y_3| + |y_1 - y_3|$. $\sqrt{s} = 7$ TeV, $\int Ldt = 4.5$ fb^{-1}.
- Asymmetric kinematics: $p_{T1} > 150$ GeV, $p_{T2} > 100$ GeV and $p_{T3} > 50$ GeV.
- NLO predictions corrected for NP effects. Several PDFs used.

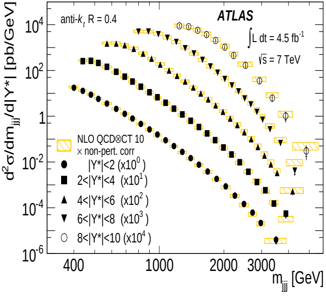

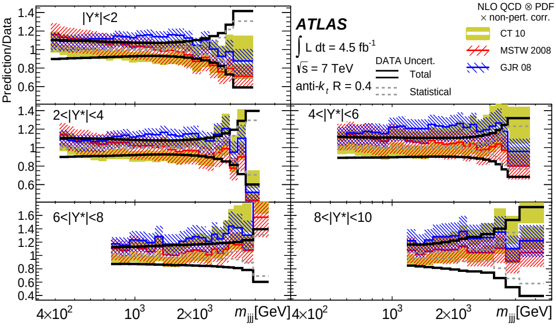

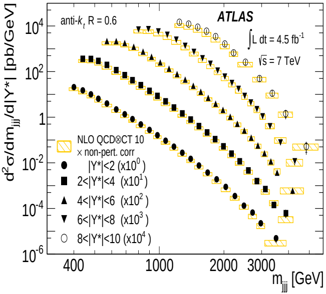

- Cross section for isolated, high-p_T photons ($E_T^{iso} \leq 7$ GeV, $E_T^{\gamma} > 100$ GeV). $\sqrt{s} = 7$ TeV, $\int Ldt = 4.6$ fb^{-1}.
- Background estimation from 2-dimensional sideband method.
- Comparison with NLO predictions by Jetphox, corrected for NP effects.

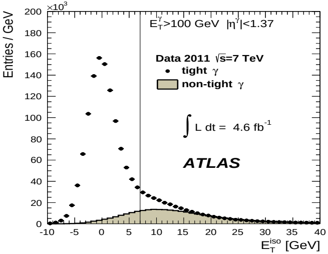

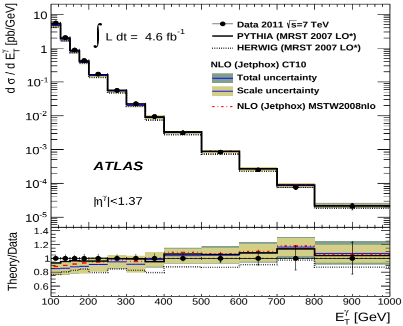

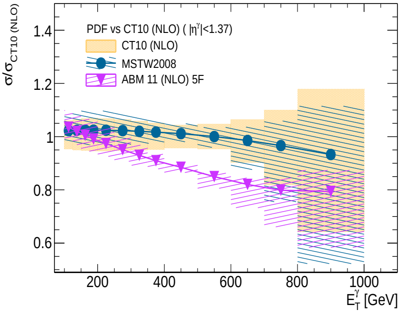

- Fraction of transverse momentum in concentric rings from the jet axis.
- Comparison of *b*-jets from $t \to Wb$ and light jets from $W \to q\overline{q'}$.
- *b*-jets have a wider distribution due to the heavier mass of the *b*-quark.

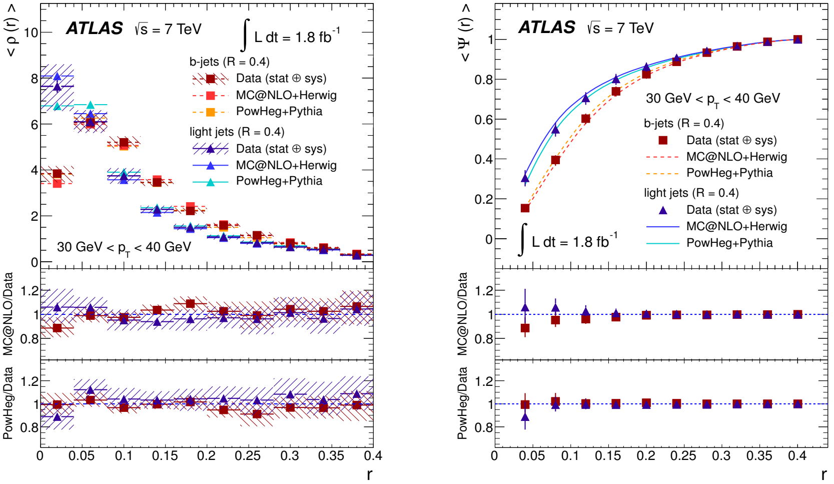

Conclusions

- QCD phenomena has been explored at ATLAS on a large energy range.
- Underlying event measurements are useful inputs for tuning the MC predictions.
- Λ polarisation and Bose-Einstein correlations follow the expectations from previous experiments.
- Jet cross-sections have been measured to a high precision for large energy ranges.
- Hard QCD measurements are well described by NLO calculations, corrected for NP (and EW) effects.
- Inclusive photon production is also well described by NLO calculations, and has sensitivity to PDF.
- Jet shapes in $t\bar{t}$ events are well described by MC expectations. Light jets have a narrower energy flow distribution than that of b-jets.
- New data at $\sqrt{s} = 13$ TeV coming soon. Stay tuned!

Backup Slides

Source	N_{ch} vs p_T^Z	$\sum p_T$ vs p_T^Z	Mean p_T vs p_T^Z	Mean p_T vs N_{ch}
Lepton selection	0.5 - 1.0	0.1 - 1.0	< 0.5	0.1 - 2.5
Track reconstruction	1.0 - 2.0	0.5 - 2.0	< 0.5	< 0.5
Impact parameter	0.5 - 1.0	1.0 - 2.0	0.1 - 2.0	< 0.5
Pile-up removal	0.5 - 2.0	0.5 - 2.0	< 0.2	0.2 - 0.5
Background correction	0.5 - 2.0	0.5 - 2.0	< 0.5	< 0.5
Unfolding	0.5 - 3.0	0.5 - 3.0	< 0.5	0.2 - 2.0
Electron isolation	0.1 - 1.0	0.5 - 2.0	0.1 - 1.5	< 1.0
Combined uncertainty	1.0 - 3.0	1.0 - 4.0	< 1.0	$1.0 - 3.5$

The distribution of the Λ decay angle from which the moments E_i are extracted for the χ^2 fit is shown below for both Λ and $\bar{\Lambda}$ baryons.

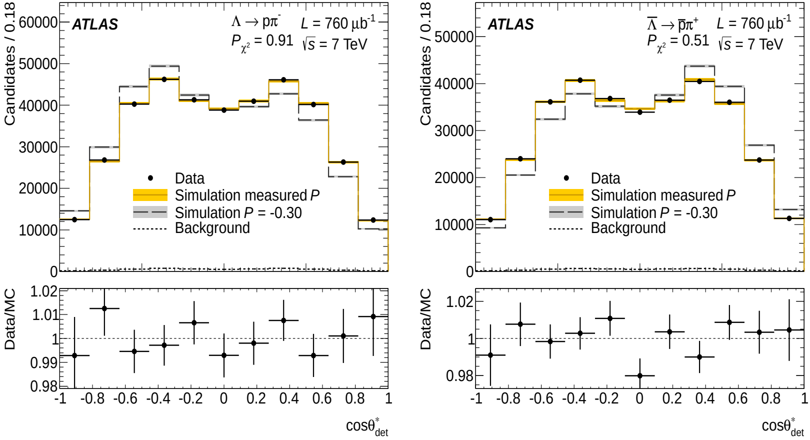

The invariant mass distribution is parameterised as a function of 11 free parameters

$$\mathcal{M}(m_{p\pi}) = f_{sig}\mathcal{M}_{sig}(m_{p\pi}) + (1 - f_{sig})\mathcal{M}_{bkg}(m_{p\pi})$$

- The signal component is

$$\mathcal{M}_{sig}(m_{p\pi}) = f_1\mathcal{G}(m_\Lambda, \sigma_1^L, \sigma_1^R) + \\ +(1 - f_1)\left[f_2\mathcal{G}(m_\Lambda, \sigma_2^L, \sigma_2^R) + \\ + (1 - f_2)\mathcal{G}(m_\Lambda, \sigma_3^L, \sigma_3^R)\right]$$

- The background component is

$$\mathcal{M}_{bkg}(m_{p\pi}) = \frac{1}{\Delta m}\left[1 + b(m_{p\pi} - m_c)\right]$$

- Signal fraction in the interval $\mathcal{I}_i$

$$f_i^{sig} = \frac{\int_{\mathcal{I}_i} \mathcal{M}_{sig}(m)dm}{\int_{\mathcal{I}_i} \mathcal{M}(m)dm}$$

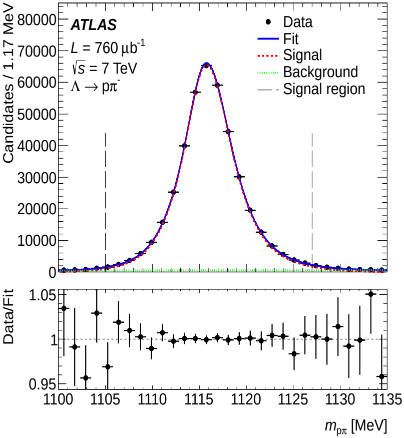

Λ polarisation. Systematic uncertainties.

The absolute systematic uncertainties for the $\Lambda/\bar{\Lambda}$ polarisation measurement are summarised below

Source	Λ	$\bar{\Lambda}$
MC statistics	0.003	0.003
Mass range	0.003	0.003
Background	0.001	0.001
Kinematic weighting	0.001	0.001
Other contributions	$< 5 \times 10^{-4}$	$< 5 \times 10^{-4}$
Total	0.004	0.004

- MC statistics: Estimated using 10 gaussian pseudoexperiments for the values of $E(0)$ and $E(1)$ in MC.
- Mass range: The signal region is varied up and down by 2 MeV.
- Background: Different background model - Uncertainties on f_i^{sig}.
- Kinematic weighting: Different weighting function for the Data - MC agreement, constructed without background subtraction.
- Other: Track momentum scale, efficiency, trigger, uncertainty in α...

Bose-Einstein correlations. λ and R versus n_{ch} and k_T.

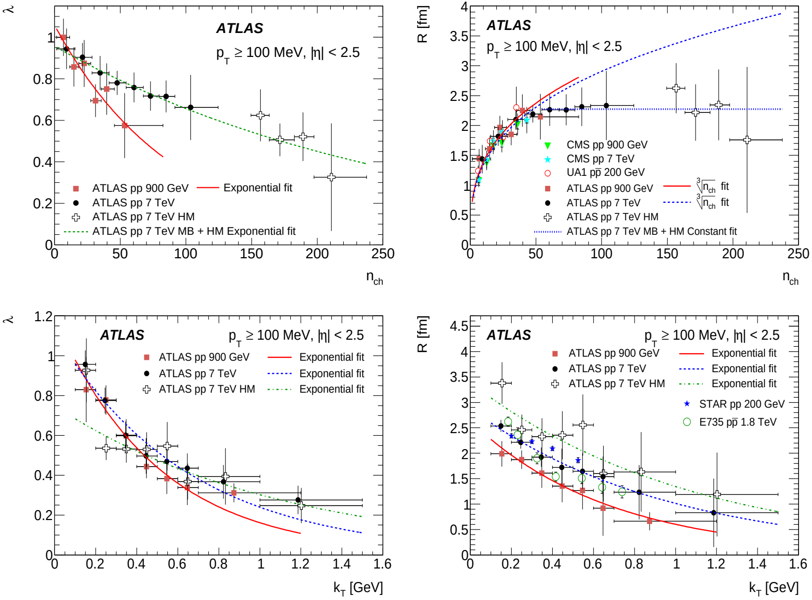

The main systematic uncertainties for the BEC measurement are shown below

	900 GeV		7 TeV		7 TeV (HM)	
Source	λ	R	λ	R	λ	R
Track efficiency	0.6%	0.7%	0.3%	0.2%	1.3%	0.3%
Splitting and merging	-	-	-	-	-	-
MC samples	14.5%	12.9%	7.6%	10.4%	5.1%	8.4%
Coulomb correction	2.6%	0.1%	5.5%	0.1%	3.7%	0.5%
Fitted range	1.0%	1.6%	1.6%	2.2%	5.5%	6.0%
Starting Q	0.4%	0.3%	0.9%	0.6%	0.5%	0.3%
Bin size	0.2%	0.2%	0.9%	0.5%	4.1%	3.4%
Exclusion interval	0.2%	0.2%	1%	0.6%	0.7%	1.1%
Total	14.8%	13.0%	9.6%	10.7%	9.4%	10.9%

Uncertainties on the gap fraction as a function of Δy and $\langle\cos(\pi - \Delta\phi)\rangle$ as a function of $\overline{p_T}$

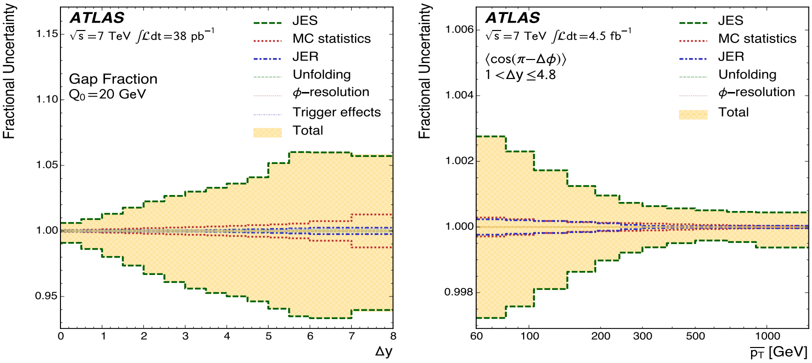

Experimental and theoretical uncertainties

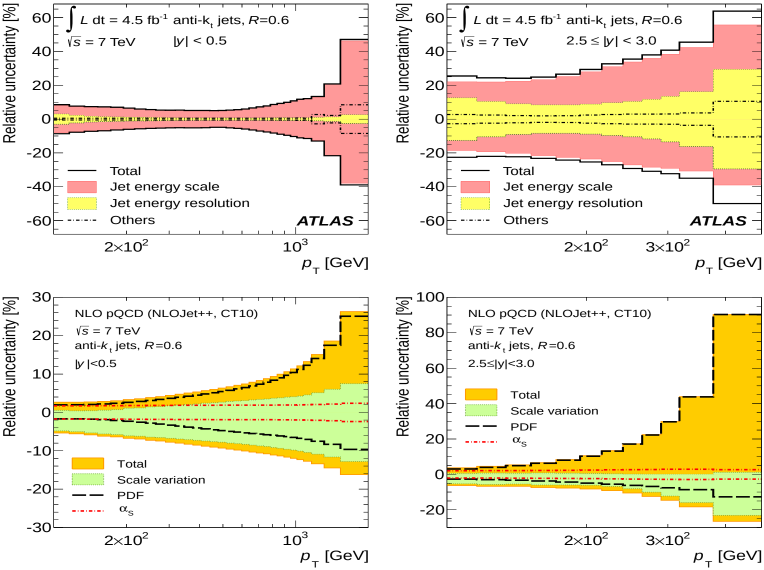

Electroweak correction factors for the cross sections with $R = 0.4$ and $R = 0.6$

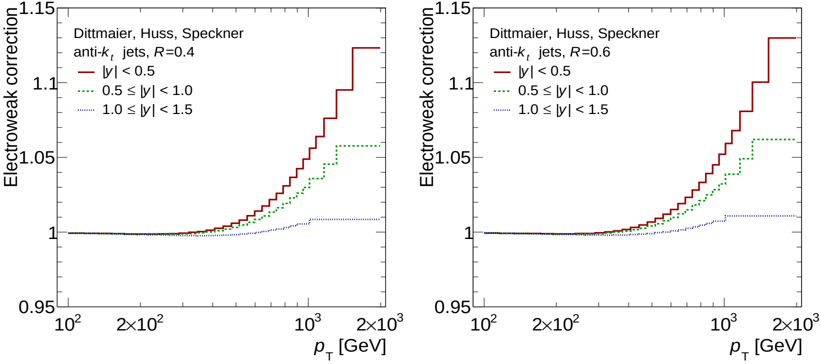

NP correction factors for $R = 0.4$ and $R = 0.6$ in the different y bins

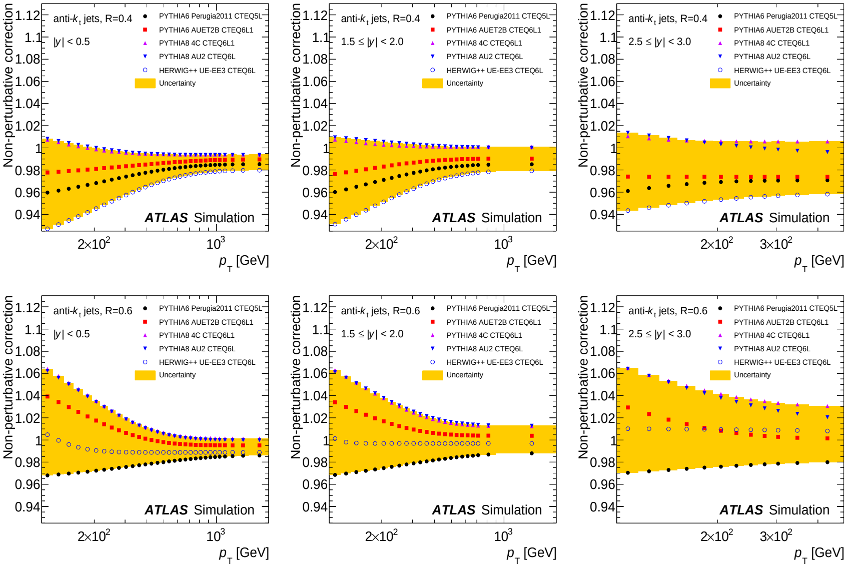

Dijet cross section. EW and NP corrections

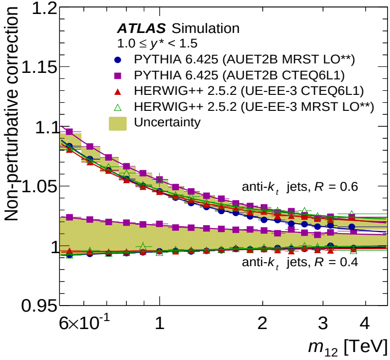

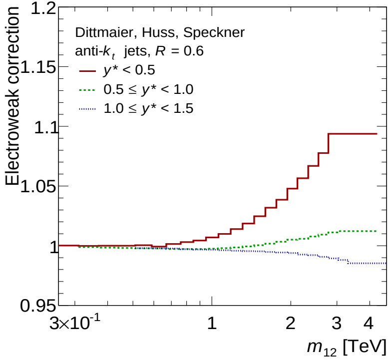

The agreement of the data with NLO pQCD predictions is tested using a χ^2 with asymmetric uncertainties.

$$\chi^2(d;t) = \min_{\beta_a} \left\{ \sum_{i,j} [d_i - F_i(\beta_a)] \left[C_{su}^{-1}(t) \right]_{ij} [d_j - F_j(\beta_a)] + \sum_a \beta_a^2 \right\}$$

$$F_i(\beta_a) = \left(1 + \sum_a \beta_a (\epsilon_a^{\pm}(\beta_a))_i \right) t_i$$

The level of agreement is quantified and contact interactions are excluded in the region $\Lambda < 7.1$ TeV.

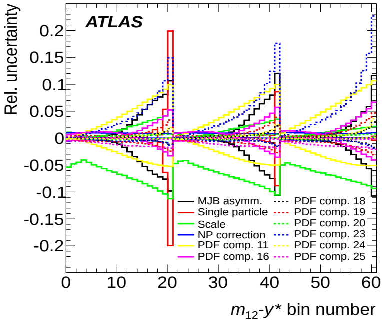

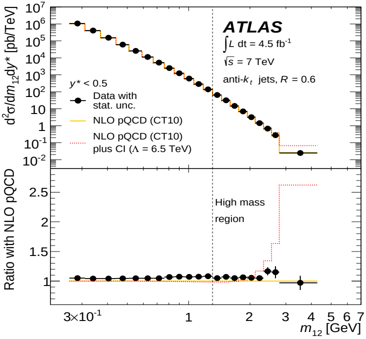

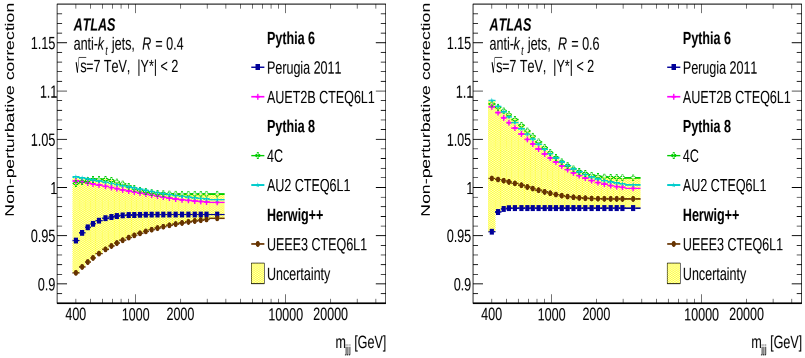
ATLAS
anti-k_t jets, R = 0.4
$\sqrt{s}$=7 TeV, |Y*| < 2
Pythia 6
Perugia 2011
AUET2B CTEQ6L1
Pythia 8
4C
AU2 CTEQ6L1
Herwig++
UEEE3 CTEQ6L1
Uncertainty
Non-perturbative correction
m_{jjj} [GeV]
ATLAS
anti-k_t jets, R = 0.6
$\sqrt{s}$=7 TeV, |Y*| < 2
Pythia 6
Perugia 2011
AUET2B CTEQ6L1
Pythia 8
4C
AU2 CTEQ6L1
Herwig++
UEEE3 CTEQ6L1
Uncertainty
Non-perturbative correction
m_{jjj} [GeV]

The observed *p*-values obtained in the comparison between data and NLO pQCD are shown below

PDF set	y^* ranges	mass range (full/high)	P_{obs} $R = 0.4$	P_{obs} $R = 0.6$
CT10	$y^* < 0.5$	high	0.742	0.785
	$y^* < 1.5$	high	0.080	0.066
	$y^* < 1.5$	full	0.324	0.168
HERAPDF 1.5	$y^* < 0.5$	high	0.688	0.504
	$y^* < 1.5$	high	0.025	0.007
	$y^* < 1.5$	full	0.137	0.025
MSTW 2008	$y^* < 0.5$	high	0.328	0.533
	$y^* < 1.5$	high	0.167	0.183
	$y^* < 1.5$	full	0.470	0.352
NNPDF 2.1	$y^* < 0.5$	high	0.405	0.568
	$y^* < 1.5$	high	0.151	0.125
	$y^* < 1.5$	full	0.431	0.242
ABM11	$y^* < 0.5$	high	0.024	$< 10^{-3}$
	$y^* < 1.5$	high	$< 10^{-3}$	$< 10^{-3}$
	$y^* < 1.5$	full	$< 10^{-3}$	$< 10^{-3}$

Three-jet cross sections. Uncertainties

Experimental and theoretical uncertainties

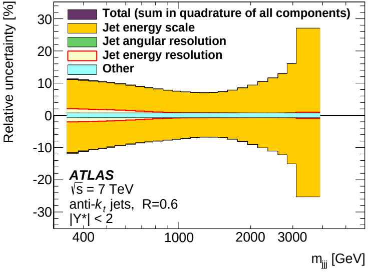

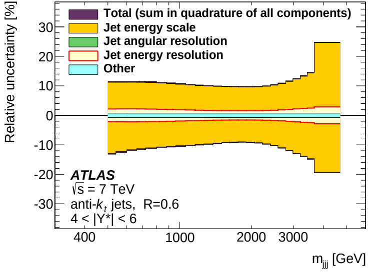

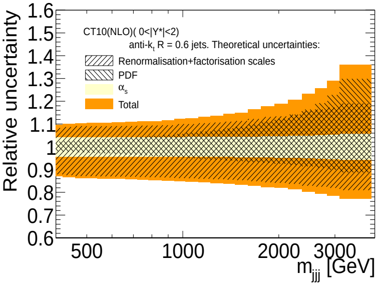

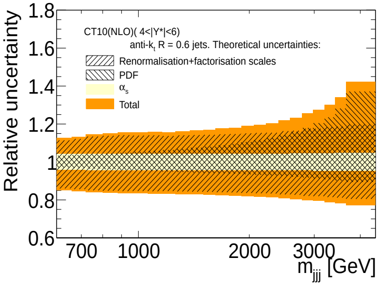

The b-jet sample is selected using b-tagging, while light jets are selected as the pair with closest mass to m_W.